# HNPS Advances in Nuclear Physics
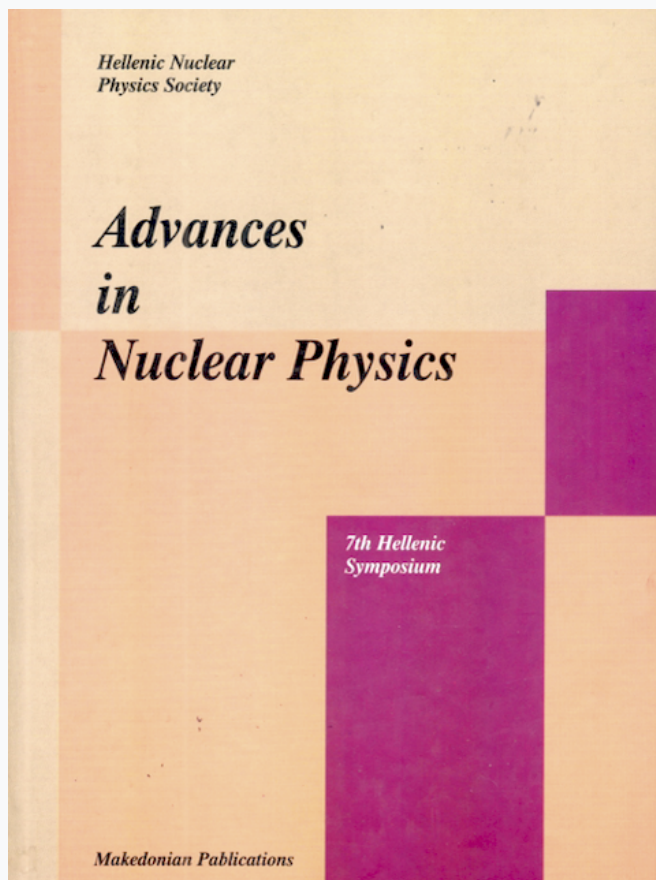
### Application of Nuclear Techniques to the Investigation of the Oxidation Behavior of Ion-Implanted Steels

F. Noli, P. Misaelides

# Application of Nuclear Techniques to the Investigation of the Oxidation Behavior of Ion-Implanted Steels

F. Noli, P. Misaelides.

*Department of Chemistry, Aristotle University, GR-54006 Thessaloniki, Greece.*

## Abstract

The oxidation behavior of ion-implanted steel samples in air, using Nuclear Reaction Analysis (NRA) and Rutherford Backscattering Spectroscopy (RBS) techniques. Austenitic stainless steel AISI 321 (Fe/Cr18/Ni8/Mn2/Ti) samples implanted with magnesium-, aluminum- and zirconium-ions (implantation energy 40 keV, dose: $1 \cdot 10^{17}$ to $2 \cdot 10^{17}$ ions/cm$^2$) were oxidized in air in the temperature region 450-650 °C for several periods of time. The above implants were selected on the basis of the affinity to oxygen, as well as their ability to form protective oxides as MgO, Al$_2$O$_3$, ZrO$_2$ in order to improve the oxidation resistance of steel. The determination of the oxygen concentration and depth-profiles was performed by means of the $^{16}$O(d, p)$^{17}$O nuclear reaction. Rutherford Backscattering Spectroscopy was applied to investigate the near-surface layers and to determine the depth profiles of the implanted ions. The determination of the aluminum concentration and the depth distribution of the Al-ions was performed using the resonance at 992 keV of the $^{27}$Al(p, $\gamma$)$^{28}$Si nuclear reaction whereas the concentration and the depth distribution of the Mg-ions by the means of the $^{24}$Mg($\alpha$, p)$^{27}$Al reaction. The excitation function of the $^{24}$Mg($\alpha$, p)$^{27}$Al nuclear reaction was studied in the energy region 4600-5000 keV and absolute cross section data allowing the determination of the Mg-profile were determined for this purpose.

## 1 Introduction

The process of thermal oxidation of the metals can be influenced by the addition of small amounts of specific reactive species affecting their surface properties [1-4]. One of the most successful techniques applied for this purpose is the ion implantation leading to the formation of thin surface layers of stable and metastable alloys. These layers show high adhesion and low porosity providing protection against oxidation and corrosion. The action of the formed protective films is due to both physical effects associated with the radiation

damage and chemical effects connected with the nature of the implanted reactive species. As criteria for the selection of the reactive elements can be used, among others, their solubility in the metal matrix, their affinity to oxygen and the formation of stable ternary oxides [5-6]. Aluminum, magnesium and zirconium exhibit high affinity to oxygen, have low solubility in iron and form stable ternary oxides, as $MgO$, $MgCr_2O_4$, $MgFe_2O_4$, $Al_2O_3$, $FeAl_2O_4$, $ZrO_2$ [7-8]. In this work the oxidation behavior of Mg-, Al- and Zr-implanted steel was studied using ion-beam analysis techniques (NRA, RBS). The modified steel samples were oxidized in air at temperatures between 450-650 °C for periods up to six days.

The $^{24}Mg(\alpha, p)^{27}Al$ nuclear reaction was studied in order to obtain absolute cross section data required for the determination of the Mg-profile.

## 2 Experimental method

Mechanically polished austenitic stainless steel AISI 321 (Fe/Cr18/Ni8/Ti) samples (supplied by Goodfellows Ltd) were implanted at room temperature under vacuum $10^{-6}$ mbar with $2 \cdot 10^{17}$ Mg- and Al-ions/cm$^2$ and $1 \cdot 10^{17}$ Zr-ions/cm$^2$. The implantations were performed using the 50 kV implanter of the Nuclear Physics Institute of the J.W. Goethe University of Frankfurt/Germany. The energy of the implantation was 40 keV and the ion beam intensity about 10 $\mu$A/cm$^2$. A liquid nitrogen trap was surrounding the target arrangement during the implantation in order to avoid the surface contamination.

The samples were oxidized in air at temperatures 450, 550 and 650 °C for periods varying from one to six days. NRA and RBS using $^4$He$^+$ particles at the 7 MeV Van de Graaf accelerator of the Nuclear Physics Institute of the University of Frankfurt were used for the investigation of the oxidized samples. The oxygen concentration was determined by the $^{16}O(d, p)^{17}O$ nuclear reaction ($E_d$=1.55 MeV, $\vartheta$=135°, $\Delta\Omega$=4.57 msr) as well as and by the 3.035 MeV resonance of the $^{16}O(\alpha, \alpha)^{16}O$ reaction ($\vartheta$=171°, $\Delta\Omega$=0.32 msr).

The distribution of the Al-ions in the near-surface layers of the material before and after the oxidation was determined using the $^{27}Al(p, \gamma)^{28}Si$ nuclear reaction and RBS whereas the depth-distribution of the Zr-ions was determined using RBS. The excitation function of the $^{24}Mg(\alpha, p)^{27}Al$ nuclear reaction, applied for the determination of the Mg-depth distribution was studied in the energy region 4600-5000 keV ($\vartheta$=158°, $\Delta\Omega$=0.87 msr).

The targets used for this work were prepared by vacuum deposition of $MgF_2$ (chemical purity 99.99%) on tantalum substrate. The thickness of the deposit-

ed material was $30\pm0.5$ $\mu g/cm^2$ determined by quartz monitoring. Mylar foils were placed in front of the detector in order to stop the backscattered alpha particles. The precision of current measurement, including the quality of the current integrator and the insulations of the Faraday cup, was about 3-7%. In order to avoid discrepancies due to the target deterioration each target was maximally irradiated with a charge of 70 $\mu$Cb. The beam energy varied between 4600 and 5000 keV.
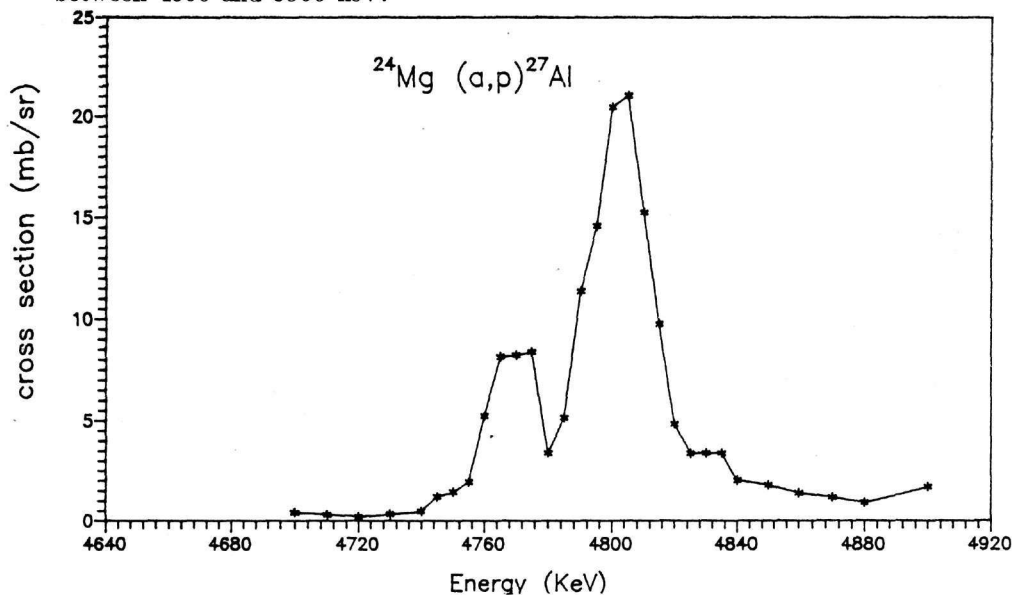


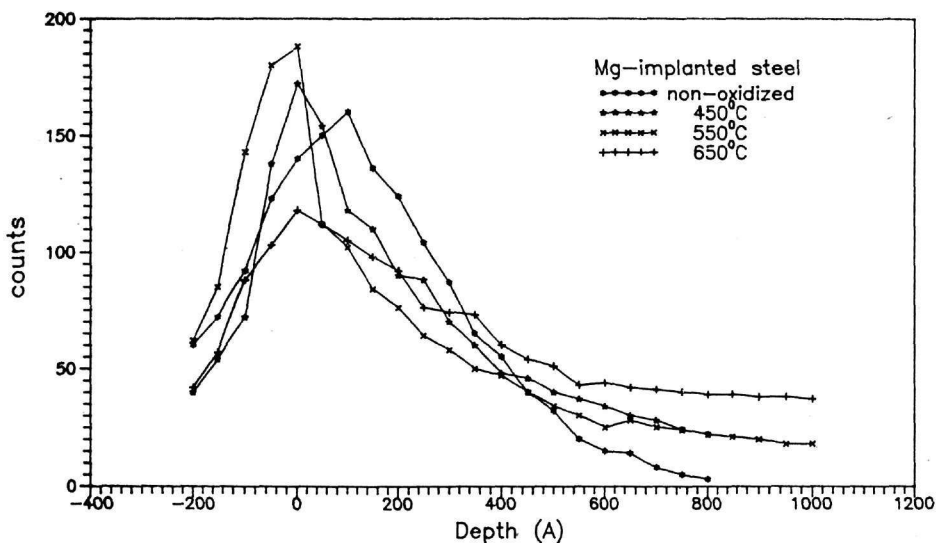Fig. 1 Cross sections of the nuclear reaction $^{24}Mg(\alpha, p)^{27}$.



Fig. 2 Distribution of 40 keV Mg-ions in AISI-321 stainless steel using the nuclear reaction $^{24}Mg(\alpha, p)^{27}$.

224

## 3    Results and discussion

The yield of the protons as a function of the bombarding energy in the region of 4700-4900 keV is given in Fig.1. Two resonances were observed in this energy region. The use of the computer code TRIM [9] made possible the theoretical determination of the Mg profile on steel. The dE/dx of helium-ions in the Mg implanted steel is 290-310 keV/$\mu$m in the energy region 4.5-5.0 MeV and the range is about 700 A as obtained using the same code. Taking into account the above data, the use of the resonance at 4805 keV enables the determination of the Mg-distribution in such a thin film without serious interference from the resonance at 4775 keV. Fig. 2 shows the Mg-profile on AISI-321 austenitic stainless steel after the implantation using the resonance at 4805 keV as well as the Mg-profiles on the Mg-implanted samples oxidized at 450, 550 and 650 °C for two days. Two different types of diffusion for the Mg-ions are indicated in the investigated temperature region (450-550 °C, diffusion towards surface and 550-650 °C, diffusion towards bulk). It was also observed that Mg-bulk diffusion takes place after oxidation at 550 °C for six days and at 650 °C. This observation was also verified by Rutherford Backscattering spectroscopy. The RBS-spectra presented in Fog. 3 correspond to Mg-implanted samples oxidized at 550 and 650 °C for two and four days respectively. The sharp peak appearing around the energy of 1.1 MeV belongs to the resonance of the $^{16}O(\alpha, \alpha)^{16}O$ reaction and the peak at the energy of 1.6 MeV to magnesium. The step appearing on the RBS-spectrum in Fig. 3b is due to the formation of a rather thick oxide layer on the sample surface. The Mg-peak in the same spectrum completely disappears because of a gradual magnesium diffusion in the bulk appearing by increasing the oxidation time and temperature.

Simulations using the computer code RUMP [10-11] provided information about the stoichiometry and the thickness of the oxide layer. At 450 °C a slight beneficial effect of the Mg-implantation was observed and the formation of a magnesium oxide layer was confirmed. At higher temperatures (550 and 650 °C), no protection against oxidation of the stainless steel was found and an intense bulk oxidation was observed leading to the formation of oxides of the steel constituents. In the implanted region the chromium concentration was found to decrease in comparison to the non-implanted. This effect connected with the Mg-bulk diffusion taking place after oxidation at high temperatures, can explain the negative role of the Mg-implantation on the oxidation behavior of the austenitic stainless steel at 550 and at 650 °C.

The oxygen distribution of the Al- and Zr-implanted and non-implanted steel samples oxidized at 650 °C is given in Fig. 4a and 4b. These data, obtained using the $^{16}O(d, p)^{17}O$ nuclear reaction, indicate, that the implantation with Al-ions significantly reduces the oxidation rate of the stainless steel whereas Zr-implanted steel is much more oxidized than the non-implanted material.

The relative RBS-spectra presented in Fig. 5 confirmed the above observations. In the spectrum of the Fig. 5b the effect of the oxidation as well as the diffusion of the Zr-ions into the steel matrix are obvious.
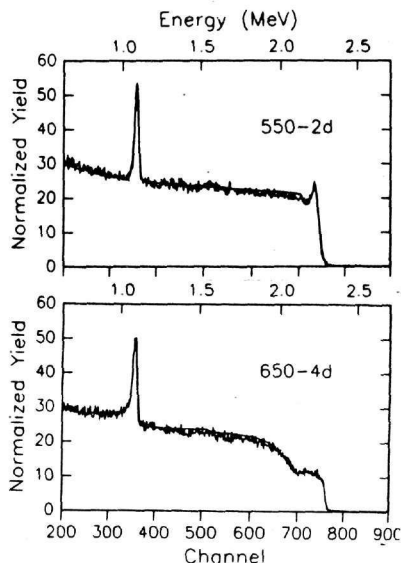


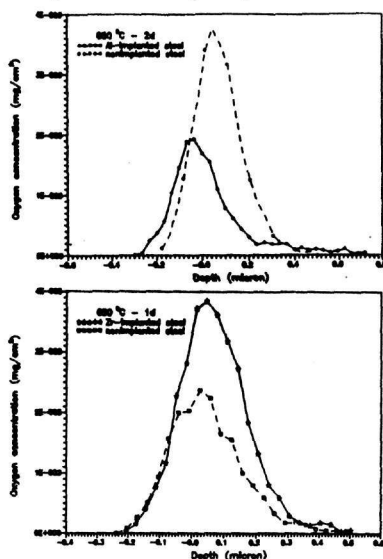Fig. 3 RBS spectra of Mg-implanted steel samples.



Fig. 4 Oxygen concentration of Al- and Zr-implanted and non-implanted steel samples oxidized at 650 °C, using the nuclear reaction $^{16}O(d, p)^{17}O$.

The Al-distribution in the implanted steel after oxidation at 450 °C for one and three days respectively is given in Fig. 6a. No significant diffusion of Al-ions appears under these experimental conditions. On the other hand the distribution of the Zr-ions presented in Fig. 6b is completely different. It seems that after oxidation at 650 °C zirconium diffuses through the bulk of the steel by

increasing the oxidation time. The investigation showed that the implantation of Al-ions in AISI 321 stainless steel leads to a significant improvement of the oxidation resistance of the material in low and in high temperatures whereas the oxidation behavior of the Zr-implanted samples seems to be affected by the oxidation time and temperature.

Aluminum because of its solubility in iron, is equally distributed between bulk and grain boundaries and blocks the sites for inward oxygen diffusion affecting both the fast diffusion paths transport and the bulk diffusion [12-14]. This is the reason for the protective role of Al-implantation on the oxidation of the stainless steel. On the other hand the limited solubility of the magnesium in iron has as result the Mg-ion diffusion through the grain boundaries from the surface into the bulk. This effect provides sites for the cation out-diffusion of iron taking place at high temperatures and explains the improvement of the oxidation resistance of the steel only at low temperatures. The oxidation behavior of Zr-implanted steel was rather complicated connected with the alteration of the Zr-diffusion type observed, as a function of the temperature and the oxidation time [15].

# 4 Conclusions

Nuclear Reaction Analysis can be successfully applied for the determination of the concentration and the depth profile of the oxygen, magnesium, aluminum and zirconium in near-surface layers of steel samples.

The determination of the concentration and the depth profile of the magnesium by means of the nuclear reaction $24Mg(\alpha, p)27Al$ showed that magnesium diffuses inward the steel by increasing the temperature. This phenomenon reduces the oxidation resistance of the Mg-implanted steel samples in high temperatures.

The Al-implantation in stainless steel leads to a significant improvement of the oxidation resistance of the material in low and in high temperatures.

The investigation of the Zr-implantation on the oxidation behavior of AISI 321 austenitic stainless steel using Nuclear Reaction Analysis, showed that the concentration and the distribution of the zirconium change varying the temperature and the oxidation time.
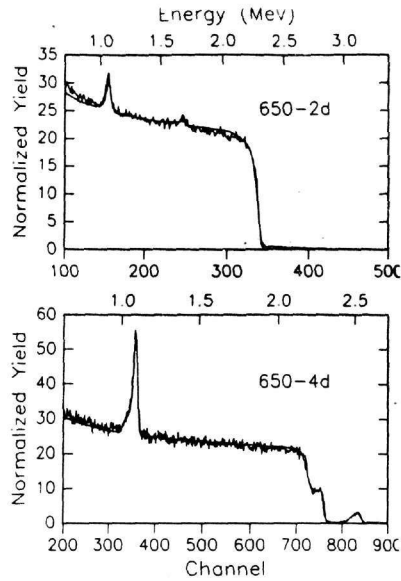
## 5  Acknowledgements

Fig. 5 RBS spectra of Al-and Zr-implanted steel samples oxidized at 650 °C.
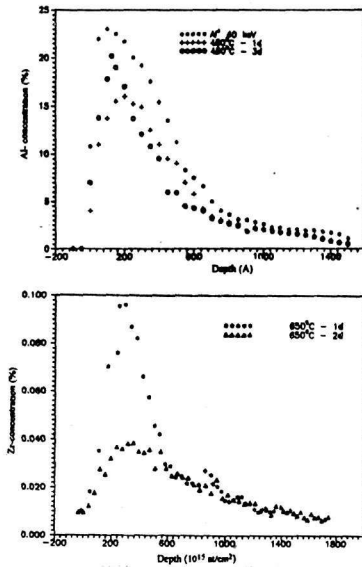


Fig. 6 Distribution of 40 keV Al- and Zr-ions in AISI-321 stainless steel using the nuclear reaction $^{27}$Al(p, $\gamma$)$^{28}$Si and RBS respectively.

228

# References

[1] M. J. Bennett, H.E. Bishop, P. R. Chalker and A. T. Tuson, *Mater. Sci. Eng.* **90**, 177 (1987).

[2] M. Pons, M. Caillet and A. Galerie, *Nucl. Instr. and Meth.* **209/210**, 1011 (1983).

[3] F. Noli, P. Misaelides, P. Spathis, M. Pilakouta and H. Baumann, *Nucl. Instr. and Meth.* **B68**, 398 (1992).

[4] F. Noli, P. Misaelides, G. Giorginis, H. Baumann and H. Hausner, *Nucl. Instr. and Meth.* **B113**, 171 (1996).

[5] W. Ensinger and G. K. Wolf, *Mat Sci. and Eng.* **A116**, 1(1989).

[6] M. Pons, M. Caillet and A. Galerie, *Defect and Diffusion Forum* **57-58**, 189 (1988).

[7] R. W. Cahn and P. Haasen, *Physical Metallurgy*, Elsevier Science Publ. 154 (1983).

[8] *Metals Handbook*, 8th edition, American Society of Metals, Metals Park, Ohio, p.1213 (1985).

[9] J. F. Ziegler and J. P. Biersack, TRIM Computer code based on The Stopping and Range of Ions in Solids, Pergamon, New York (1985).

[10] L. R. Doolittle, Computer code RUMP based on: Algorithms of the Rapid Simulation of Rutherford Backscattering Spectra, *Nucl. Instr. and Meth.* **B9**, 344 (1985).

[11] L. R. Doolittle, Computer code RUMP based on: Algorithm for Rutherford Backscattering Analysis, *Nucl. Instr. and Meth.* **B15**, 227 (1986).

[12] R. Molins, J. D. Bartout and Y. Bienvenu, *Mater. Sci. and Eng.* **A135**, 111 (1991).

[13] A. Galerie, *Ion Implantation into Metals*, Pergamon, Oxford, p. 190 (1982).

[14] C. I. Howe, B. McEnaney, V. D. Scott and G. Dearnaley, *Ion Implantation into Metals*, Pergamon, Oxford, p.211 (1982).

[15] G. Dearnaley, *Nucl. Instr. and Meth.* **182/183**, 899 (1982).